Synthesis and application of TiO_2 single-crystal nanorod arrays grown by multicycle hydrothermal for dye-sensitized solar cells*

Zhu Jian-Jing(朱建晶), Zhao Yu-Long(赵宇龙)†, Zhu Lei(朱 磊), Gu Xiu-Quan(顾修全), and Qiang Ying-Huai(强颖怀)

School of Materials Science and Engineering, China University of Mining and Technology, Xuzhou 221116, *China*

(Received 13 August 2013; revised manuscript received 9 October 2013; published online 20 February 2014)

TiO_2 is a wide band gap semiconductor with important applications in photovoltaic cells. Vertically aligned TiO_2 nanorod arrays (NRs) are grown on the fluorine-doped tin oxide (FTO) substrates by a multicycle hydrothermal synthesis process. The samples are characterized by X-ray diffraction (XRD), scanning electron microscopy (SEM), high-resolution transmission electron microscopy (HRTEM), and selected-area electron diffraction (SAED). It is found that dye-sensitized solar cells (DSSCs) assembled by the as-prepared TiO_2 single-crystal NRs exhibit different trends under the condition of different nucleation and growth concentrations. Optimum cell performance is obtained with high nucleation concentration and low growth cycle concentration. The efficiency enhancement is mainly attributed to the improved specific surface area of the nanorod.

Keywords: TiO_2 single-crystal nanorod array, mild multicycle hydrothermal, dye-sensitized solar cell, low growth cycle concentration

PACS: 81.10.Aj, 68.55.–a, 42.25.Bs, 81.07.Gf **DOI:** 10.1088/1674-1056/23/4/048104

1. Introduction

Dye-sensitized solar cells (DSSCs) have aroused widespread interest due to their low production cost and relatively high energy conversion efficiencies.[1,2] A typical DSSC consists of a photoanode covered by dye molecules, an electrolyte normally containing I^-/I_3^- redox couple, and a Pt thin film counter electrode. TiO_2 mesoporous film with a large surface area of the traditional photoanode material and a power conversion efficiency of 12.3% has been achieved in a recent report.[3] However, in spite of having a high surface area, mesoporous film has a low electron transport rate due to the grain boundaries of the interconnected nanoparticles.[4,5] In recent years, one-dimensional (1D) nanostructured material with a high aspect ratio, such as nanorods/nanowires, has dimensionality-dependent and size reduction-dependent electrical and thermal transport or mechanical properties.[6] Compared with other 1D nanomaterials, TiO_2 nanorod/nanowire array is very promising photoanode material for the rapid charge transport and the good optical transmittance with an increased incident light intensity on the N719 dye.[7,8] Much effort has recently been made to optimize the nanostructured electrode for DSSCs, such as synthesizing branched structures, doping or coating with metal oxide,[9–11] improving preparation method,[12,13] increasing the light path length and the light absorptance of dye sensitizer,[14] using different materials,[15] depositing a seed layer to control the morphology,[16,17] composite photoelectrodes, and preparing single-crystal nanorod arrays.[18,19]

TiO_2 single-crystal nanorod arrays (NRs) have a higher electron diffusion coefficient, more than two orders of magnitude higher than that of rutile nanoparticle film, and can suppress the recombination of charge carriers with redox species. However, lower conversion efficiency has been obtained because of the smaller surface area of TiO_2 single-crystal NRs, which resulted in low dye adsorption. It can enlarge the surface area by increasing the length of TiO_2 NRs,[20] but at the same time TiO_2 NRs will turn wide, too. Besides, there will be fusion phenomenon between the bottom of TiO_2 NRs,[21] which will lead to lower surface area.

In this article, we try to prepare single-crystal NRs by multiple growth cycles. The TiO_2 NRs nucleate in high concentration, and grow in low concentration, which maybe reduces the fusion of NRs. By investigating the relationship between the efficiencies of different growth cycle times, we find that different growth cycle times, nucleation, and growth concentration actually exhibit different photoelectrical performances.

2. Experiment

2.1. Synthesis of TiO_2 NRs

The single-crystal TiO_2 NRs were prepared using hydrothermal synthesis method reported previously.[22] In a typical synthesis, 15-mL deionised water was mixed with 15-mL hydrochloric acid (HCl, 37 wt%) and stirred for 5 min. 0.5-mL tetrabutyl titanate was added dropwise to the above mixture and stirred for another 5 min to obtain a clear solution.

*Project supported by the Fundamental Research Funds for the Central Universities, China (Grant No. 2013XK07).

†Corresponding author. E-mail: sdyulong@cumt.edu.cn

© 2014 Chinese Physical Society and IOP Publishing Ltd

The F-doped SnO_2 (FTO) glass ($\sim$ 2-mm thick) was ultrasonically cleaned in the mixed solution of 10-mL acetone, 10-mL isopropyl alcohol and 10-mL deionized water for 30 min, then cleaned with deionized water again and dried in ambient air. The FTO substrate was placed horizontally in a teflon autoclave (60 mL in volume), and the precursor solution was added to it. The teflon autoclave was then sealed and heated to 150 °C for different growth times in an oven. After synthesis, the autoclave was cooled to room temperature, the FTO substrate was taken out, rinsed extensively with distilled water and heated in air at 500 °C for 30 min.

To obtain the cycle growth nanorod arrays, a multistep hydrothermal growth process was employed as follows: we placed the FTO substrate obtained from the first step in another reactor filled with freshly prepared growth solution, and heated at 150 °C for another 4 h. This process may be repeated multiple times to obtain the wanted TiO_2 single-crystal NRs.

2.2. Fabrication of DSSC

To assemble DSSCs, the as-synthesized and sintered TiO_2 NRs were immersed in 0.3-mM ethanolic solution of N719 over 24 h to absorb the dye at room temperature. A platinum-coated FTO substrate was used as a counter electrode. Then, the dye-sensitized electrode, together with counter electrode, were assembled into a sandwich-type cell using a thermal-plastic spacer (DHS-SN1760, 60-μm thickness). The spacing between the electrodes was filled with ionic electrolyte solution by capillary to complete the cell fabrication. The electrolyte contained 0.6-M 1-butyl-3-methylimidazolium iodide, 0.03-M I_2, 0.5-M tert-butylpyridine, and 0.1-M guanidinium thiocyanate in acetonitrile/valeronitrile 85/15(volume).

2.3. Characterization and measurement

The morphologies and crystal structures of the TiO_2 nanorods were characterized by field emission scanning electron microscope (FESEM, Sirion 200) and X-ray diffraction (XRD, D8 Advance, Bruker, Germany) with a Cu Kα radiation source ($\lambda = 1.54$ Å). The current density–voltage (J–V) measurements were carried out by a digital Keithley 2420 source meter under AM 1.5G irradiation with 100-mW/cm^2 light intensity. The simulated sunlight was provided by a 500-W xenon lamp equipped with an AM 1.5 fitter (Newport Oriel Sol3A, 94023). The illumination intensity of 100 mW/cm^2 was calibrated with a standard monocrystalline silicon solar cell which passed the American Society for Testing and Materials (ASTM) calibration. The active cell area was fixed to be 0.20 cm^2 by a light shading mask.

3. Results and discussion

Figure 1 displays the XRD patterns of the as-prepared TiO_2 NRs. The dominant (002) peak indicates that the nanorods are well crystallized and highly oriented. TiO_2 nanorods grow in the [001] direction with the growth axis parallel to the substrate. Figure 2(a) is FESEM image, which clearly shows the view of TiO_2 in nucleation initial stage; this image also reveals the feasibility of TiO_2 nanorod nucleating in a high concentration. The nanrods are monocrystalline, which is confirmed by HR-TEM and SAED images shown in Fig. 2(b). High-resolution TEM and SAED images indicate that TiO_2 nanorods are monocrystalline with the growth direction along $\langle 001 \rangle$. Figure 2(b) also shows the cross-sectional SEM images of the standard monocrystal TiO_2 NRs. The average diameter and length of the nanorods are 100 nm and 2 μm, respectively, and the nanorods are highly oriented with respect to the substrate.

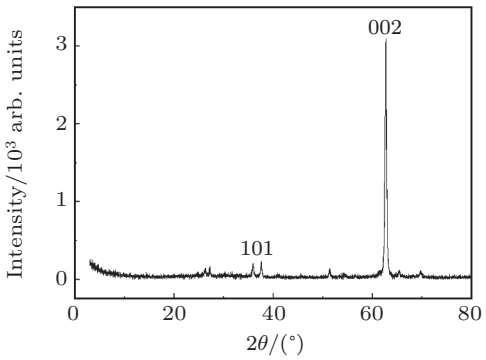


Fig. 1. XRD pattern (0.5-mL tetrabutyl titanate, 22 h).

Our research shows that increasing titanium precursor concentration and times of cycle growth could significantly enhance the length of nanorod arrays. Figure 2(c) shows the FESEM image of TiO_2 nanorod arrays grown with 1.5-mL tetrabutyl titanate. When titanium precursor concentration increases from 0.4 mL to 1.5 mL, dandelion-type structure NRs, with 7 μm in length and 240 nm$\sim$600 nm in diameter, are formed. Figure 2(d) shows the FESEM image of TiO_2 NRs with 16 times of cycle growth, the average length and diameter of nanorods reach 15 μm and 200 nm, respectively. Although the above NRs have the length values of 7 μm and 15 μm, they each have a poor power conversion efficiency due to fusion phenomenon.

Liu and Eray[23] showed that the NRs would be loose in a low titanium precursor concentration. When the titanium precursor concentration is low, the nanorods are not aligned for the low nucleation density. Our results show that NRs cannot nucleate on the FTO when 0.3-mL tetrabutyl titanate is used, but in this concentration, the NRs could grow if a seed layer has formed on the substrate. So nucleating in a high concentration and growing in a low concentration may obtain loose NRs.

Figures 3(a)–3(d) show the cross-sectional TiO_2 NRs by multiple growth cycles: 2, 4, 6, 8 times with 0.4-mL tetrabutyl titanate. With the number of times of cycle increasing,

the nanorods become longer and longer. The length values of nanorods can reach 0.8 μm, 1.2 μm–1.5 μm, 1.5 μm–1.8 μm, 2 μm–2.3 μm, respectively. Simultaneously, the diameters of nanorods become bigger and bigger, the diameter values reach 80 nm–100 nm, 100 nm–150 nm, 150 nm–250 nm, 250 nm–270 nm, respectively. From Fig. 2 we can find that as the number of times of cycle increases, the number of the nanorods in the unit area increases. The number and density of nanorods increase as the reaction proceeds, the high nucleation density promotes the generating of new nanorods. The increase in the number of nanorods induces the nanorods to approach each other. As a result, the TiO_2 nanorods are fused at their roots.

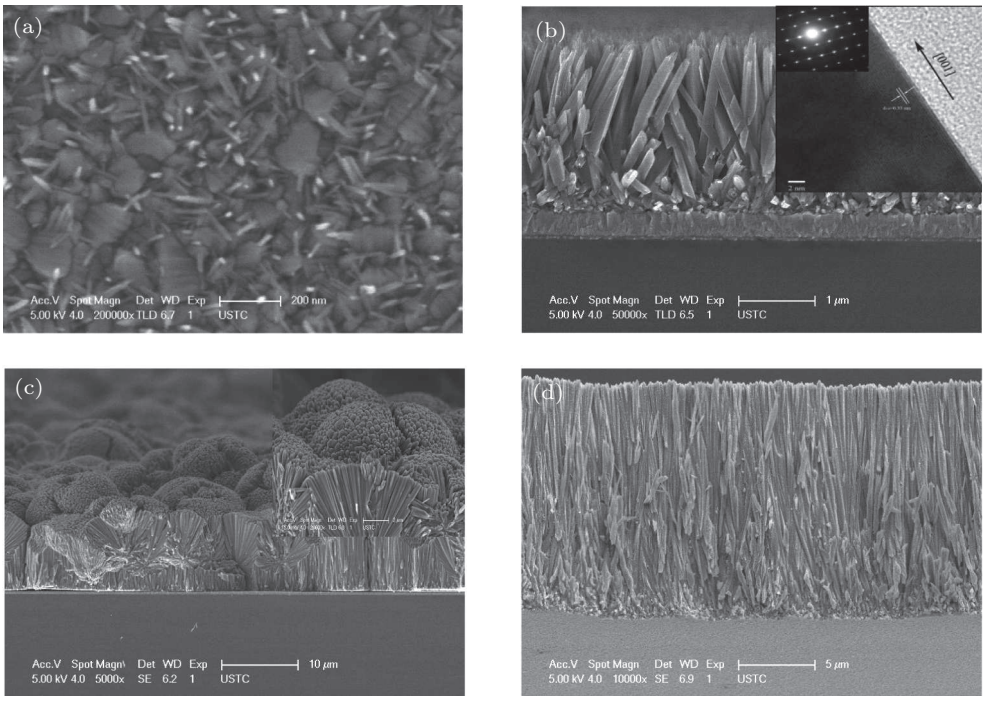


Fig. 2. (a) FESEM image (0.5-mL tetrabutyl titanate, 2 h). (b) SEM and TEM images (0.4-mL tetrabutyl titanate, 22 h). (c) SEM image (1.5-mL tetrabutyl titanate, 13 h). (d) SEM image of cycling 16 times (0.4-mL tetrabutyl titanate).

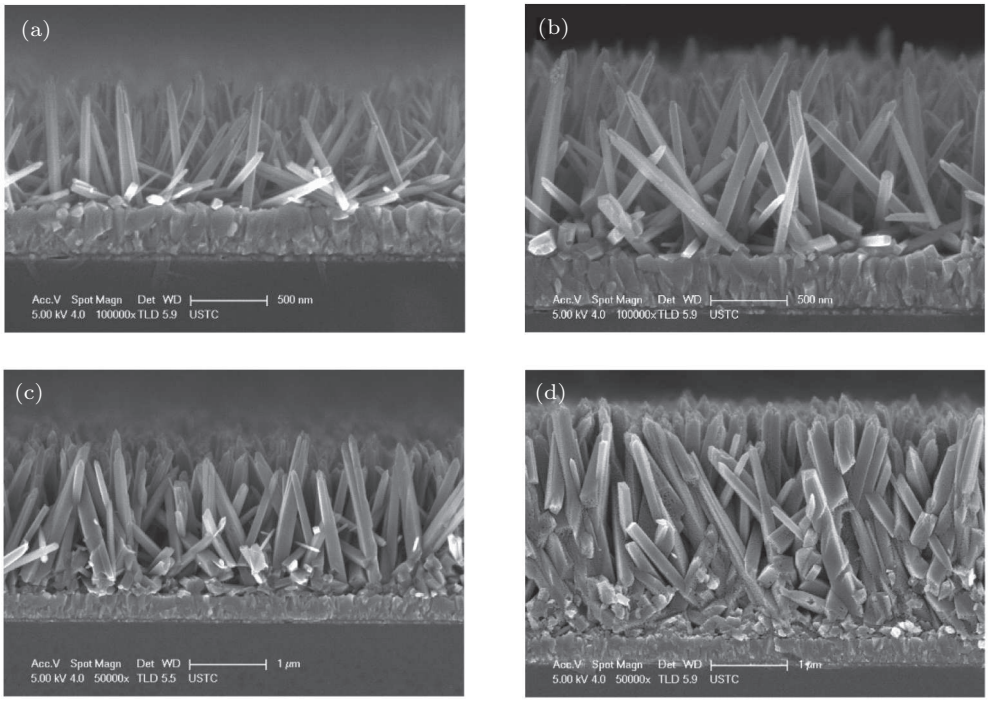


Fig. 3. SEM images of (a) 2 times of growth cycle, (b) 4 times of growth cycle, (c) 6 times of growth cycle, and (d) 8 times of growth cycle.

Figure 4 shows the SEM images of TiO_2 nanorods on FTO by multiple growth cycles, and using 0.5-mL nucleation concentration, 0.3-mL cycle growth concentration. With the number of times of cycle increases, the length values of nanorods reach 1.5 μm–1.7 μm, 2 μm–2.2 μm, 2.3 μm–2.5 μm, 2.7 μm–2.9 μm, respectively. The diameter values of the nanorods reach 100 nm–150 nm, 180 nm–200 nm, 200 nm–250 nm, and 250 nm–300 nm. In the later growth stage, there is no apparent increase in the number of the nanorods. With these methods, we can still not obtain incompact nanorods. Although the density of the nanorods does not increase too much, the TiO_2 nanorods fused at their roots form a continuous film due to an increase in the lateral dimension.[24]

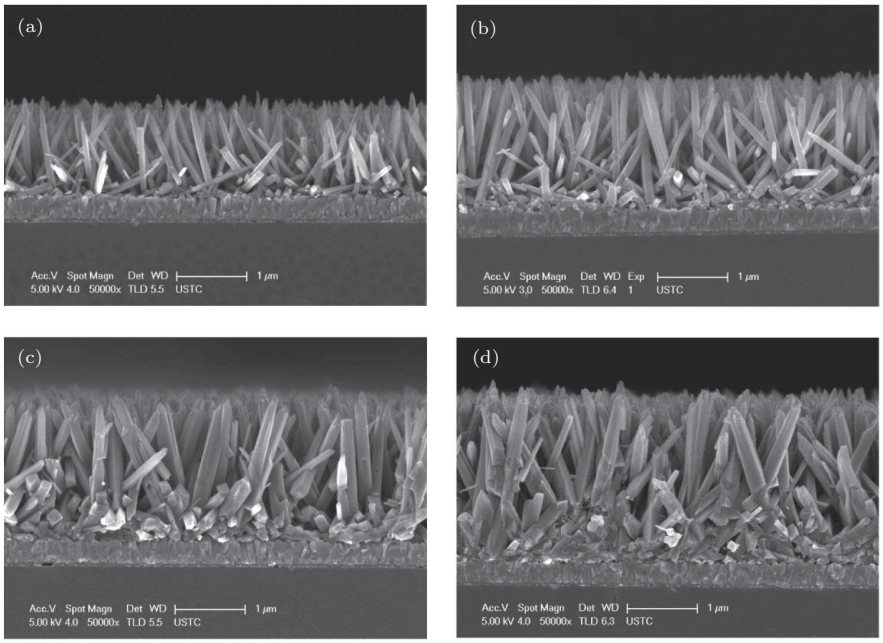


Fig. 4. SEM images of (a) 2 times of growth cycle, (b) 4 times of growth cycle, (c) 6 times of growth cycle, and (d) 8 times of growth cycle.

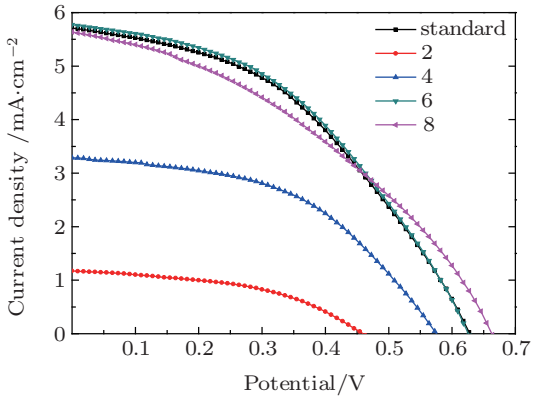


Fig. 5. (color online) Curves of current density versus voltage of DSSCs composed of as-grown TiO_2 NR arrays with different growth cycles and using 0.4-mL titanium precursor concentration.

Figures 5 and 6 show the J–V characteristic curves of DSSCs based on the different growth cycles under AM 1.5 sunlight illumination (100 mW/cm^2). The performances are shown in Table 1, from which we can see the performances of DSSCs assembled with TiO_2 NRs by hydrothermal growth of different times. From Fig. 5 and Table 1, we can find the current density, fill factor, and conversion efficiency first increase and then decrease, the open-circuit voltage increases constantly, when the cycle times reach 6, 0.4-mL cycle growth has a short-circuit current (J_{SC}) of 5.77 mA/cm^2 and an open-circuit voltage (V_{OC}) of 0.63 V, which exhibits the best performance with an overall power conversion efficiency (η) of 1.57%. This is because when the number of times of growth cycle reaches 6, the length-diameter ratio of the nanorod is suitable, 8 times of growth cycle can increase the length values of the nanorods, but the TiO_2 nanorods will be fused at their roots, which is due to the number of the nanorods. These will lead to poorer performances.

Table 1. Performances of DSSC composed of the as-prepared TiO_2 NR arrays with different numbers of times of growth cycle.

Growth condition	J_{SC}/mA·cm^{-2}	V_{OC}/V	FF	η/ %
standard 0.4	4.39	0.64	0.55	1.53
2 cycles 0.4	1.19	0.46	0.44	0.25
4 cycles 0.4	3.25	0.58	0.48	0.91
6 cycles 0.4	5.77	0.63	0.44	1.57
8 cycles 0.4	5.61	0.66	0.39	1.43
2 cycles 0.5, 0.3	4.12	0.64	0.47	1.22
4 cycles 0.5, 0.3	6.50	0.67	0.40	1.92
6 cycles 0.5, 0.3	5.86	0.65	0.42	1.59
8 cycles 0.5, 0.3	5.99	0.66	0.40	1.58

From Fig. 6 and Table 1, we can find the J_{SC} and conversion efficiency also first increase and then decrease on the whole. Because the 0.5-mL nucleation concentration is high, the roots of the nanorods become more compact, 0.3-mL cycle growth concentration will not continue to nucleate, so the taller part of the nanorods are loose. When the number of times of growth cycle reaches 4, 0.3-mL cycle growth has a short-circuit current (J_{SC}) of 6.50 mA/cm^2 and an open-circuit voltage (V_{OC}) of 0.67 V, which exhibits the best performance with an overall power conversion efficiency (η) of 1.92%. Nanorods are formed during the first stage, as growth time increases, the number and length values of the nanorods all reach a right scope, after 4 times of growth cycle, although the length values of the nanorods increase, the lateral dimension increases distinctly, the nanorods are fused on the FTO substrate, and the compact nanorod will reduce the performances of the DSSC.

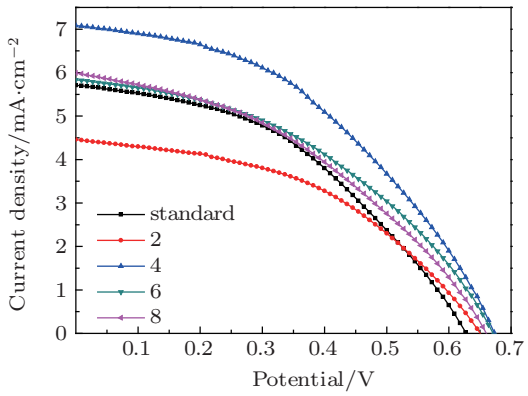


Fig. 6. (color online) Curves of current density versus voltage of DSSCs composed of as-grown TiO_2 NR arrays with different growth cycles, and using 0.5-mL nucleation concentration, 0.3-mL cycle growth concentration.

Comparison among different concentration growth cycles shows that the low concentration growth cycles display the better cell performance. Low concentration growth cycle can obtain higher cell performance due to the nanorods being longer and loosely arranged, low concentration growth cycle also has a low radial growth diameter, the nanorods can be longer before the nanorods get compact. But high concentration growth cycle can cause the new nanorods to nucleate and grow, the nanorods will get compact before the nanorods reach a long length. Low concentration growth cycle can control the number of the nanorods and improve the cell performance, but this method cannot restrain the increase of diameter and the thin film becomes compact.

4. Conclusion

In this paper, the TiO_2 nanorods are successfully prepared by a mild multicycle hydrothermal synthesis process. The importance of the number of times of TiO_2 nanorod growth cycle, nucleation concentration, and cycle growth concentration is investigated. The prepared DSSC shows a conversion efficiency $\sim 1.92\%$ by 4 times of growth cycle with 0.5-mL nucleation concentration, 0.3-mL cycle growth concentration. Although TiO_2 single-crystal nanorods have many advantages, the roots of the nanorods still become compact, which leads to lower surface area, the conversion efficiency will be influenced. The further improvement in the cell efficiency should be possible with incompact and long nanorods.

References

[1] O'Regan B and Grätzel M 1991 *Nature* **353** 737
[2] Law M, Greene L E, Johnson J C, Saykally R and Yang P 2005 *Nat. Mater.* **4** 455
[3] Yella A, Lee H W, Tsao H N, Yi C Y, Chandiran A K, Nazeeruddin M K, Diau E W G, Yeh C Y, Zakeeruddin S M and Grätzel M 2011 *Science* **334** 629
[4] Fisher A C, Peter L M, Ponomarev E A, Walker A B and Wijayantha K G U 2000 *J. Phys. Chem. B* **104** 949
[5] Bisquert J, Cahen D, Hodes G, Ruhle S and Zaban A 2004 *J. Phys. Chem. B* **108** 8106
[6] Qin Z H 2013 *Chin. Phys. B* **22** 098108
[7] Liao J Y, Lei B X, Chen H Y, Kuang D B and Su C Y 2012 *Energy Environ. Sci.* **5** 5750
[8] Shao F, Sun J, Gao L, Yang S W and Luo J Q 2012 *J. Mater. Chem.* **22** 6824
[9] Xu M, Da P M, Wu H Y, Zhao D Y and Zheng G F 2012 *Nano Lett.* **12** 1503
[10] Feng X J, Shankar K, Paulose M and Grimes C A 2009 *Angew. Chem. Int. Ed.* **48** 8095
[11] Barea E, Xu X Q, Gonzalez-Pedro V, Ripolles-Sanchis T, Fabregat-Santiago F and Bisquert J 2011 *Energy Environ. Sci.* **4** 3414
[12] Yang M J, Ding B, Lee S and Lee J K 2011 *J. Phys. Chem. C* **115** 14534
[13] Huang Q L, Zhou G, Fang L, Hu L P and Wang Z S 2011 *Energy Environ. Sci.* **4** 2145
[14] Xiong B T, Zhou B X, Bai J, Zheng Q, Liu Y B, Cai W M and Cai J 2008 *Chin. Phys. B* **17** 3713
[15] Li Y, Jia X P, Hu M H, Liu X B, Yan B M, Zhou Z X, Zhang Z F and Ma H A 2012 *Chin. Phys. B* **21** 058101
[16] Sun P P, Zhang X T, Liu X P, Wang L L, Wang C H, Yang J K and Liu Y C 2012 *J. Mater. Chem.* **22** 6389
[17] Park J T, Patel R, Jeon H, Kim D J, Shin J S and Kim J H 2012 *J. Mater. Chem.* **22** 6131
[18] Ai G, Sun W T, Zhang Y L and Peng L M 2011 *Chem. Commun.* **47** 6608
[19] Dai G T, Zhao L, Li J, Wan L, Hu F, Xu Z X, Dong B H, Lu H B, Wang S M and Yu J G 2012 *J. Colloid Interface Sci.* **365** 46
[20] Zhao Y L, Gu X Q and Qiang Y H 2012 *Thin Solid Films* **520** 2814
[21] Kumar A, Madaria A R and Zhou C W 2010 *J. Phys. Chem. C* **114** 7787
[22] Kumar A, Li K T, Madaria A R and Zhou C W 2011 *Nano Res.* **4** 1181
[23] Liu B and Aydil E S 2009 *J. Am. Chem. Soc.* **131** 3985
[24] Zhou Z J, Fan J Q, Wang X, Zhou W H, Du Z L and Wu S X 2011 *ACS Appl. Mater. Interfaces* **3** 4349